Acta Crystallographica Section B
Structural Science
ISSN 0108-7681

Structure, phase transitions and ionic conductivity of $K_3NdSi_6O_{15}\cdot xH_2O$. II. Structure of β-$K_3NdSi_6O_{15}$

S. M. Haile[a]* and B. J. Wuensch[b]

[a]Materials Science, California Institute of Technology, Pasadena, CA 91125, USA, and [b]Department of Materials Science and Engineering, Massachusetts Institute of Technology, Cambridge, MA 02139-4307, USA

Correspondence e-mail: smhaile@caltech.edu

Received 12 May 1999
Accepted 6 December 1999

Hydrothermally grown crystals of β-$K_3NdSi_6O_{15}$, potassium neodymium silicate, have been studied by single-crystal X-ray methods. Under appropriate conditions, the compound crystallizes in space group $Bb2_1m$ and has lattice constants a = 14.370 (2), b = 15.518 (2) and c = 14.265 (2) Å. There are 30 atom sites in the asymmetric unit of the basic structure. With eight formula units per unit cell, the calculated density is 2.798 Mg m^{-3}. Refinement was carried out to a residual, $wR(F^2)$, of 0.1177 [$R(F)$ = 0.0416] using anisotropic temperature factors for all atoms. The structure is based on $(Si_2O_5^{2-})_\infty$ layers, connected by Nd polyhedra to form a three-dimensional framework. Potassium ion sites, some of which are only partially occupied, are located within channels that run between the silicate layers. The silica–neodymia framework of β-$K_3NdSi_6O_{15}$, in particular the linkages formed between the silicate layers and Nd polyhedra, bears some similarities to that of the essentially isocompositional phase α-$K_3NdSi_6O_{15}\cdot 2H_2O$. In both, the silicate layers are corrugated so as to accommodate a simple cubic array of NdO_6 octahedra with lattice constant $\sim$ 7.5 Å. Furthermore, the Si_2O_5 layers in β-$K_3NdSi_6O_{15}$ are topologically identical to those of the mineral sazhinite, $Na_2HCeSi_6O_{15}$. Although β-$K_3NdSi_6O_{15}$ and sazhinite are not isostructural, the structures of each can be described as slight distortions of a high-symmetry parent structure with space group *Pbmm*.

1. Introduction

The present paper is the second in a two-part series describing the structure and physical properties of $K_3NdSi_6O_{15}\cdot xH_2O$, and is part of a broad effort to elucidate the relationship between structure and ion transport in alkali rare-earth silicates. Such compounds provide broad possibilities for crystal-chemical tailoring of their properties *via* independent chemical substitutions on the alkali, rare-earth and even Si-atom sites. In part I of this series (Haile & Wuensch, 2000) a reanalysis of the structure of α-$K_3NdSi_6O_{15}\cdot 2H_2O$ is presented, a compound first reported by (Pushcharovskii *et al.*, 1981), along with selected physical properties. In particular, conductivity and structural phase transformations are described. In the present paper we report the structure of a new, anhydrous polymorph, β-$K_3NdSi_6O_{15}$.

2. Experimental

2.1. Crystal growth

Crystals of β-$K_3NdSi_6O_{15}$ were obtained from hydrothermal experiments carried out isothermally. The conditions that led to the crystallization of β-$K_3NdSi_6O_{15}$ were a temperature of

Table 1
Experimental details.

Crystal data	
Chemical formula	β-$K_3NdSi_6O_{15}$
Chemical formula weight	670
Cell setting	Orthorhombic
Space group	$Bb2_1m$
a (Å)	14.370 (2)
b (Å)	15.518 (2)
c (Å)	14.265 (2)
V (Å^3)	3181.0 (7)
Z	8
D_x (Mg m^{-3})	2.798
Radiation type	Mo $K\alpha$
Wavelength (Å)	0.71073
No. of reflections for cell parameters	22
μ (mm^{-1})	4.310
Temperature (K)	293 (2)
Crystal size (mm)	0.3 × 0.3 × 0.2
Data collection	
Diffractometer	Siemens $R3m$/V
Absorption correction	ψ scan (empirical)
T_{min}	0.057
T_{max}	0.119
No. of measured reflections	1975
No. of independent reflections	1975
No. of observed reflections	1952
Criterion for observed reflections	$I \geq 2\sigma$
θ_{max} (°)	27.50
Range of h, k, l	$0 \rightarrow h \rightarrow 18$ $0 \rightarrow k \rightarrow 20$ $0 \rightarrow l \rightarrow 18$
Deviation of standards from initial value min/max/mean/final	0.9887/1.0353/1.0160/1.0137
No. of standard reflections	69
Refinement	
Refinement on	F^2
$R[F^2>2\sigma(F^2)]$	0.0416
$wR(F^2)$	0.1177
S	1.129
No. of reflections used in refinement	1974
No. of restraints used	1
No. of parameters used	244
Weighting scheme	$w = 1/[\sigma^2F_o^2 + (0.0746P)^2 + 44.0045P]$, where $P = [\max(F_o^2,0) + 2F_c^2]/3$
$(\Delta/\sigma)_{max,mean}$	0.177, 0.0011
$\Delta\rho_{max}$ (e Å^{-3})	2.593
$\Delta\rho_{min}$ (e Å^{-3})	−1.762
Extinction method	None
Absolute structure parameter	0.10 (3)
Source of atomic scattering factors	Cromer & Waber (1974)
Computer programs	
Structure refinement	*SHELXL* (Sheldrick, 1993)

773 K, a pressure of 82.5 MPa (controlled explicitly) and a synthesis period of 5 d. The precursor material was a glass of composition 4 K_2O–Nd_2O_3–17SiO_2 and the solvent either deionized water or water containing up to 2*M* KOH. Further details of the synthesis are given elsewhere (Haile *et al.*, 1993). As noted in Part I of this series, the hydrothermal conditions described above led, in most cases, to the crystallization of α-$K_3NdSi_6O_{15}\cdot 2H_2O$ rather than β-$K_3NdSi_6O_{15}$. Indeed, the β form of $K_3NdSi_6O_{15}\cdot xH_2O$ was obtained from only the first three of well over 100 experiments carried out in the high silica region of the SiO_2–Nd_2O_3–K_2O system. The observation that the α and β forms of $K_3NdSi_6O_{15}\cdot xH_2O$ crystallized under ostensibly identical hydrothermal conditions suggests that the energetic difference between the two phases is quite small. This conclusion is further supported by the similarity of their crystal structures, as discussed below.

Table 2
Atomic coordinates of β-$K_3NdSi_6O_{15}$.

The compound crystallizes in space group $Bb2_1m$, and has lattice constants a = 14.370 (2), b = 15.518 (2) and c = 14.265 (7) Å.

Atom	Position	Symmetry	x	y	z
Nd(1)	8(*b*)		0.49154 (3)	0.57468 (6)	0.76341 (3)
Si(1)	8(*b*)		0.3846 (2)	0.7537 (2)	0.6119 (2)
Si(2)	8(*b*)		0.6157 (2)	0.4554 (2)	0.6051 (2)
Si(3)	8(*b*)		0.3352 (2)	0.7146 (2)	0.8969 (2)
Si(4)	8(*b*)		0.7796 (2)	0.4854 (2)	0.7495 (2)
Si(5)	8(*b*)		0.6511 (2)	0.4129 (2)	0.8930 (2)
Si(6)	8(*b*)		0.7284 (2)	0.6711 (2)	0.7837 (2)
K(1)†	8(*b*)		0.4616 (2)	0.3182 (2)	0.7854 (3)
K(2)†	4(*a*)	..*m*	0.5754 (3)	0.6302 (4)	0
K(3)†	4(*a*)	..*m*	0.8658 (4)	0.4920 (3)	1/2
K(4)	4(*a*)	..*m*	0.8725 (3)	0.5194 (4)	0
K(5)	4(*a*)	..*m*	0.5896 (3)	0.6691 (3)	1/2
K(6)‡	4(*a*)	..*m*	0.8463 (10)	0.3053 (11)	1/2
O(1)	8(*b*)		0.7874 (5)	0.5821 (6)	0.7990 (5)
O(2)	8(*b*)		0.4057 (6)	0.8563 (5)	0.6299 (6)
O(3)	8(*b*)		0.3788 (6)	0.8116 (5)	0.8869 (5)
O(4)	8(*b*)		0.6974 (7)	0.4919 (7)	0.6720 (6)
O(5)	4(*a*)	..*m*	0.6849 (8)	0.4354 (8)	0
O(6)	8(*b*)		0.8790 (6)	0.4633 (5)	0.7096 (7)
O(7)	4(*a*)	..*m*	0.7856 (8)	0.7081 (7)	1/2
O(8)	8(*b*)		0.9570 (6)	0.6962 (5)	0.8319 (6)
O(9)	8(*b*)		0.1215 (5)	0.6630 (6)	0.6951 (6)
O(10)	4(*a*)	..*m*	0.8906 (9)	0.7351 (9)	0
O(11)	8(*b*)		0.7482 (6)	0.4201 (6)	0.8321 (6)
O(12)	8(*b*)		0.4142 (5)	0.6453 (5)	0.1137 (6)
O(13)	4(*a*)	..*m*	0.6607 (8)	0.4602 (9)	1/2
O(14)	8(*b*)		0.5710 (6)	0.4750 (5)	0.8597 (7)
O(15)	8(*b*)		0.2239 (6)	0.2381 (6)	0.8582 (6)
O(16)	8(*b*)		0.2509 (6)	0.2046 (6)	0.6766 (6)
O(17)	8(*b*)		0.5265 (7)	0.5127 (6)	0.6165 (6)

† Occupancy fixed at 0.94. ‡ Occupancy fixed at 0.24.

2.2. Composition determination

The composition of crystals obtained from the hydrothermal experiments was determined from electron microprobe measurements. Crystals (identified by single-crystal methods to be of the desired phase) were mounted in an epoxy resin and coated with carbon by evaporation. Data were collected on a Jeol Superprobe 733 equipped with a wavelength dispersive detector. The intensities of the characteristic X-radiation peaks were converted to stoichiometric quantities using the *ZAF* data reduction program (Schamber *et al.*, 1981). The following materials were employed as standards: enstatite ($Mg_2Si_2O_6$) for silicon, single crystal $NdGaO_3$ for neodymium and amorphous K feldspar ($KAlSi_3O_8$) for potassium. These measurements yielded mole percentages of K, Nd and Si of 6.3 (5), 4.00 (8) and 26.3 (4) mol%, respectively. Relative to that for ideal $K_3NdSi_6O_{15}$ (12, 4 and 24 mol%, respectively) the measured composition appears to be deficient in potassium. However, measurements of α-$K_3NdSi_6O_{15}\cdot 2H_2O$, the

Table 3
Thermal parameters of β-$K_3NdSi_6O_{15}$.

Anisotropic temperature factors are of the form: $\exp[-2\pi^2(h^2u^{11}a^{*2}+\ldots+hku^{12}a^*b^*+\ldots)]$ and are given in units of 10^{-2} Å^2. U_{iso} is $1/3(U^{11}+U^{22}+U^{33})$.

Atom	U_{iso}	U^{11}	U^{22}	U^{33}	U^{23}	U^{13}	U^{12}
Nd(1)	1.61 (2)	1.72 (2)	1.31 (3)	1.79 (3)	0.05 (3)	−0.07 (2)	0.14 (3)
Si(1)	1.73 (5)	1.91 (13)	1.34 (12)	1.93 (13)	0.11 (10)	0.05 (10)	0.01 (10)
Si(2)	1.79 (6)	2.06 (14)	1.51 (13)	1.80 (13)	−0.10 (10)	−0.14 (10)	0.03 (11)
Si(3)	1.66 (5)	1.73 (12)	1.37 (12)	1.86 (13)	0.04 (10)	0.01 (10)	0.06 (10)
Si(4)	1.74 (6)	1.77 (14)	1.57 (14)	1.88 (12)	−0.10 (10)	−0.01 (11)	−0.09 (13)
Si(5)	1.86 (6)	1.86 (13)	1.58 (13)	2.14 (14)	0.32 (11)	−0.02 (11)	−0.15 (11)
Si(6)	1.69 (5)	1.65 (13)	1.62 (13)	1.80 (12)	−0.08 (11)	0.00 (12)	−0.02 (11)
K(1)	3.54 (7)	2.56 (13)	2.03 (13)	6.0 (2)	−0.52 (14)	0.5 (2)	−0.03 (11)
K(2)	3.38 (9)	2.9 (2)	5.0 (3)	2.2 (2)	0	0	−0.6 (2)
K(3)	4.09 (11)	5.7 (3)	3.2 (2)	3.3 (2)	0	0	−1.1 (2)
K(4)	5.08 (12)	2.8 (2)	6.5 (3)	6.0 (3)	0	0	−0.1 (2)
K(5)	4.99 (13)	2.9 (2)	3.9 (2)	8.2 (4)	0	0	0.3 (2)
K(6)	2.7 (3)	1.5 (6)	3.6 (8)	3.0 (7)	0	0	0.0 (6)
O(1)	2.4 (2)	2.6 (3)	1.8 (3)	2.7 (4)	−1.1 (4)	−0.7 (3)	−0.3 (4)
O(2)	2.6 (2)	2.9 (4)	1.4 (3)	3.6 (5)	0.2 (3)	−0.5 (4)	0.1 (3)
O(3)	2.1 (2)	2.9 (4)	0.6 (3)	2.8 (4)	−0.3 (3)	0.3 (3)	−0.3 (3)
O(4)	3.4 (2)	3.9 (5)	3.8 (5)	2.6 (4)	0.1 (4)	−1.2 (4)	−1.4 (4)
O(5)	2.4 (2)	2.5 (6)	2.7 (6)	2.1 (5)	0	0	0.1 (5)
O(6)	2.8 (2)	2.2 (4)	1.9 (4)	4.3 (5)	−0.5 (4)	1.6 (4)	−0.2 (3)
O(7)	2.0 (2)	2.0 (5)	1.5 (5)	2.4 (5)	0	0	0.0 (4)
O(8)	2.2 (2)	2.6 (4)	1.2 (3)	2.8 (4)	−0.7 (3)	0.3 (3)	0.2 (3)
O(9)	2.3 (2)	1.8 (3)	2.6 (4)	2.6 (4)	−0.2 (3)	0.0 (3)	−0.2 (3)
O(10)	2.7 (3)	3.2 (6)	3.4 (7)	1.6 (5)	0	0	0.7 (5)
O(11)	2.4 (2)	1.9 (4)	2.3 (4)	3.0 (4)	0.8 (3)	0.4 (3)	0.3 (3)
O(12)	1.9 (2)	1.8 (3)	1.4 (3)	2.6 (4)	0.0 (3)	−0.4 (3)	0.2 (3)
O(13)	2.6 (3)	1.9 (5)	4.2 (8)	1.9 (5)	0	0	0.3 (5)
O(14)	2.7 (2)	2.2 (4)	1.8 (4)	4.0 (5)	0.5 (4)	−0.1 (4)	0.0 (3)
O(15)	2.4 (2)	1.7 (4)	2.3 (4)	3.2 (4)	−1.0 (4)	0.3 (3)	−0.1 (3)
O(16)	2.3 (2)	2.2 (4)	2.4 (4)	2.1 (4)	0.6 (3)	−0.6 (3)	−0.2 (3)
O(17)	2.9 (2)	3.9 (5)	3.0 (5)	1.9 (4)	−0.6 (3)	0.0 (4)	1.2 (4)

stoichiometry of which was well established, yielded similarly alkali-poor results (Haile & Wuensch, 2000). Conversion of the experimental mol% values of the metals to the weight percentages of the respective oxides yields a sum of 99.0 (6) wt%.

2.3. Structure determination

Single-crystal X-ray intensity data were collected with Mo $K\alpha$ radiation (λ = 0.71073 Å) at room temperature using a Siemens *R*3*m*/*V* diffractometer. Refinement of the lattice parameters, using data for the positions of 22 peaks, revealed β-$K_3NdSi_6O_{15}$ to be B-centered orthorhombic with lattice constants a = 14.370 (2), b = 15.518 (2) and c = 14.265 (2) Å. Complete crystal data and details of the diffraction data collection are given in Table 1.

Systematic absences showed the diffraction symbol to be *Bb***, permitting $Bb2_1m$, *Bb*2*m* and *Bbmm* as possible space groups. The value of $|E^2-1|$ was 0.660, suggesting a non-centrosymmetric structure, and, in the final stages of the refinement, $Bb2_1m$ proved to be the correct space group on the basis of the reasonableness of calculated bond lengths and the magnitude of the residuals.

The structure was solved by first locating the Nd, Si and most K atoms by direct methods using the *SHELXS*86 program (Sheldrick, 1985). The lighter oxygen atoms and partially occupied potassium sites were located from iterative Fourier difference maps. Structure-factor calculations and least-squares refinement were carried out using the *SHELXL*93 program (Sheldrick, 1993), and, accordingly, a residual based on F^2 values was minimized, and only one very negative reflection [$I < -2\sigma(I)$] was omitted. The handedness of the structure was determined by comparing the refinements of both the structure determined initially and its inverse. In addition, the possibility of racemic twinning was examined by the method of Flack (Bernardinelli & Flack, 1985), which involves a floating point origin and the constrained refinement of the *y*-coordinates of all atoms. Further discussion is provided below. The final residuals, obtained using anisotropic thermal parameters for all atoms, are given in Table 2. Calculated and observed F^2 have been deposited.[1] The atomic coordinates and thermal parameters are provided in Tables 2 and 3, respectively. The interatomic distances and angles in the Nd and Si coordination polyhedra are given in Table 4. Oxygen atoms which are bonded to two silicon atoms are given the subscript 'br' to denote that they 'bridge' two tetrahedral groups and those that are bonded to only one are given the subscript 't' to indicate that they 'terminate' a tetrahedral group. These latter atoms are also referred to as 'apical' in the text. The distances between potassium ions and their anion neighbors are presented in Table 5. For the present purposes, nearest-anion neighbors to potassium ions are defined as those which are closer to the potassium than its nearest Si or Nd neighbor, which ranged from 3.455 Å for K(1) to 3.851 Å for K(4). Anion next-nearest neighbors are defined as those at distances up to 4.0 Å from potassium.

The handedness represented by the coordinates in Table 2, which we hereby refer to as right-handed, was taken to correctly describe the structure because it provided more reasonable Nd—O bond distances than its inverse. In both cases, the average Nd—O distance was 2.37 Å, however, for the right-handed structure the difference between the shortest and longest distances was $\sim$ 0.06 Å compared with $\sim$ 0.11 Å

[1] Supplementary data for this paper are available from the IUCr electronic archives (Reference: BS0008). Services for accessing these data are described at the back of the journal.

Table 4
Interatomic distances and bond angles in the neodymium and silicon coordination polyhedra in β-$K_3NdSi_6O_{15}$.

Atom		Bond distance (Å)	Oxygen separation along edge (Å)		O—*M*—O angle (°)
Nd(1)	$O(12)^{i}$	2.348 (8)	O(12)—O(14)	3.494 (11)	95.8 (3)
	O(17)	2.360 (9)	O(12)— O(8)	3.270 (12)	87.6 (3)
	O(14)	2.363 (8)	O(12)—O(9)	3.209 (11)	85.3 (3)
	$O(8)^{ii}$	2.378 (8)	O(12)—O(6)	3.179 (12)	84.1 (3)
	$O(9)^{iii}$	2.390 (8)	O(17)—O(14)	3.575 (13)	98.4 (3)
	$O(6)^{ii}$	2.398 (9)	O(17)—O(8)	3.107 (12)	82.0 (3)
			O(17)—O(9)	3.810 (13)	106.7 (3)
			O(17)—O(6)	3.351 (14)	89.6 (4)
			O(14)—O(9)	3.106 (12)	81.6 (3)
			O(14)—O(6)	2.936 (12)	76.1 (3)
			O(8)—O(9)	3.108 (11)	81.4 (3)
			O(8)—O(6)	4.168 (12)	121.5 (3)
	Average	2.37 (2)		3.4 (4)	91 (13)
			Transpolyhedral angles		
			O(12)—O(17)		162.6 (3)
			O(14)—O(8)		162.3 (3)
			O(9)—O(6)		154.2 (3)
Si(1)	$O(8)_t^{ii}$	1.587 (8)	O(8)—O(2)	2.647 (11)	110.2 (5)
	$O(10)_{br}^{iv}$	1.624 (4)	O(8)—O(10)	2.651 (10)	111.3 (6)
	$O(15)_{br}^{v}$	1.635 (8)	O(8)—O(15)	2.705 (11)	114.2 (5)
	$O(2)_{br}$	1.640 (9)	O(10)—O(15)	2.608 (12)	106.3 (6)
			O(10)—O(2)	2.649 (13)	108.5 (6)
			O(15)—O(2)	2.620 (12)	106.2 (5)
Si(2)	$O(17)_t$	1.568 (9)	O(17)—O(2)	2.622 (12)	111.3 (5)
	$O(2)_{br}^{vi}$	1.609 (9)	O(17)—O(4)	2.600 (14)	109.5 (5)
	$O(4)_{br}$	1.615 (9)	O(17)—O(13)	2.673 (13)	113.2 (6)
	$O(13)_{br}$	1.635 (6)	O(2)—O(4)	2.643 (13)	110.1 (5)
			O(2)—O(13)	2.636 (13)	108.7 (6)
			O(4)—O(13)	2.557 (10)	103.8 (5)
Si(3)	$O(12)_t^{i}$	1.571 (8)	$O(12)^{ii}$—O(16)	2.699 (11)	115.0 (5)
	$O(16)_{br}^{v}$	1.629 (8)	O(12)—O(3)	2.630 (10)	110.2 (4)
	$O(3)_{br}$	1.636 (8)	O(12)—O(7)	2.645 (12)	111.0 (5)
	$O(7)_{br}^{iv}$	1.638 (6)	O(16)—O(3)	2.655 (11)	108.8 (5)
			O(16)—O(7)	2.574 (9)	104.0 (5)
			O(3)—O(7)	2.641 (12)	107.5 (2)
Si(4)	$O(6)_t$	1.577 (8)	O(6)—O(11)	2.653 (12)	112.2 (5)
	$O(11)_{br}$	1.619 (9)	O(6)—O(4)	2.702 (14)	115.3 (6)
	$O(4)_{br}$	1.621 (10)	O(6)—O(1)	2.600 (12)	106.8 (5)
	$O(1)_{br}$	1.662 (9)	O(11)—O(4)	2.644 (13)	109.4 (5)
			O(11)—O(1)	2.621 (13)	106.0 (5)
			O(4)—O(1)	2.630 (12)	106.5 (5)
Si(5)	$O(14)_t$	1.575 (9)	O(14)—O(3)	2.665 (11)	112.4 (4)
	$O(3)_{br}^{vi}$	1.633 (8)	O(14)—O(5)	2.658 (12)	111.6 (6)
	$O(5)_{br}^{vii}$	1.639 (5)	O(14)—O(11)	2.714 (12)	114.7 (5)
	$O(11)_{br}$	1.647 (9)	O(3)—O(5)	2.671 (13)	109.4 (5)
			O(3)—O(11)	2.603 (11)	105.1 (5)
			O(5)—O(11)	2.573 (10)	103.1 (5)
Si(6)	$O(9)_t^{iii}$	1.571 (8)	O(9)—O(1)	2.696 (12)	114.4 (5)
	$O(1)_{br}$	1.636 (10)	O(9)—O(15)	2.622 (11)	109.6 (5)
	$O(15)_{br}^{viii}$	1.637 (9)	O(9)—O(16)	2.670 (11)	112.5 (5)
	$O(16)_{br}^{viii}$	1.641 (8)	O(1)—O(15)	2.568 (13)	103.4 (4)
			O(1)—O(16)	2.639 (13)	107.3 (4)
			O(15)—O(16)	2.670 (12)	109.1 (5)

$\langle Si—O_t \rangle$ = 1.633 (13), $\langle Si—O_{br} \rangle$ = 1.575 (9), $\langle O—O \rangle$ = 2.64 (4) Å, $\langle O—Si—O \rangle$ = 109 (3)°. Symmetry codes: (i) $x, y, -z+1$; (ii) $x-\frac{1}{2}, y, -z+\frac{3}{2}$; (iii) $x+\frac{1}{2}, y, -z+\frac{3}{2}$; (iv) $x-\frac{1}{2}, y, z+\frac{1}{2}$; (v) $-x+\frac{1}{2}, y+\frac{1}{2}, -z+\frac{3}{2}$; (vi) $-x+1, y-\frac{1}{2}, z$; (vii) $x, y, z+1$; (viii) $-x+1, y+\frac{1}{2}, z$. Atomic nomenclature: t = terminal; br = bridging.

for the inverse. In contrast, the Si—O bond distances obtained with the two models were within one standard deviation of one another. The influence of the handedness on the Nd—O bond distances resulted from the fact that, in addition to inversion, the two refined models differed in the placement of the Nd atom relative to the remainder of the structure by 0.0016 in the *y*-coordinate. In light of this, it is not surprising that attempts to refine a model in which the crystal was presumed to be composed of two inversely related twins resulted in an unacceptably high correlation between the neodymium *y*-coordinate and the twin weight. Furthermore, and again not surprisingly, as the weight of the left-handed twin was increased, the distortion of the NdO_6 polyhedron increased. The twin model was therefore rejected and the coordinates given in Table 2 settled upon.

As indicated in Table 2, in addition to one neodymium, six silicon and 17 oxygen sites, the structure of β-$K_3NdSi_6O_{15}$ contains six potassium sites in the asymmetric unit, four of which are less than fully occupied. Refinement of a structural model that contained only five, but fully occupied potassium sites, K(1)–K(5), proceeded to a residual of $wR(F^2) \simeq 0.14$ [$R(F) \simeq 0.049$]. An electron density difference map revealed significant residual electron density at two sites, the first with 6.7 e Å^{-3} and the latter with 2.5 e Å^{-3}. In the case of α-$K_3NdSi_6O_{15}\cdot 2H_2O$ similar sites were assumed to be occupied by water molecules. In the present compound, however, assignment of H_2O to these positions, while providing residuals slightly improved over those listed in Table 2, implied a stoichiometry much richer in water than determined from the compositional analysis. Furthermore, the volume per formula unit in β-$K_3NdSi_6O_{15}$ is 397.63 (9) Å^3, compared with 437.10 (8) Å^3 for α-$K_3NdSi_6O_{15}\cdot 2H_2O$ (Haile & Wuensch, 2000), suggesting that the present compound should have fewer atoms in the formula unit. Accordingly, the electron density at the first site was taken to be due to potassium, the site identified as K(6), and its partial occupation accompanied by the reduction in the occupancies of neighboring potassium sites, specifically, K(1), K(2) and K(3). The occupancies at these four sites were subsequently refined under the constraints that the occupancies of the first three [K(1), K(2)

Table 5
Distances in α-$K_3NdSi_6O_{15}\cdot 2H_2O$ between potassium ions and their nearest neighbors, and between potassium ions and their next-nearest oxygen neighbors.

K(1) neighbor	Distance (Å)	K(2) neighbor	Distance (Å)	K(3) neighbor	Distance (Å)
O(6)^{i}	2.546 (9)	O(12)^{ii}	2.837 (9)	K(6)	2.91 (2)
O(9)^{iii}	2.702 (9)	O(12)	2.837 (9)	O(12)^{iv}	2.962 (8)
O(3)^{v}	2.714 (9)	O(9)^{vi}	2.906 (9)	O(12)^{vii}	2.962 (8)
O(8)^{vii}	2.784 (9)	O(9)^{vii}	2.906 (9)	O(13)	2.988 (13)
O(2)^{v}	2.984 (9)	K(6)^{viii}	2.94 (2)	O(6)^{ix}	3.029 (11)
O(14)	3.085 (9)	O(14)^{x}	3.133 (10)	O(6)	3.029 (11)
K(6)^{xi}	3.486 (8)	O(14)^{ix}	3.133 (10)	O(4)^{ix}	3.447 (11)
Next neighbor		O(5)	3.408 (13)	O(4)	3.447 (11)
O(12)^{xii}	3.529 (8)	K(3)^{xiii}	3.697 (7)	O(7)	3.546 (12)
O(15)	3.780 (9)	Next neighbor		O(14)^{xiv}	3.574 (10)
O(16)	3.831 (9)	O(15)^{xv}	3.900 (10)	O(14)^{vi}	3.574 (10)
O(11)^{i}	3.835 (9)	O(15)^{xvi}	3.900 (9)	K(2)^{iv}	3.697 (7)
O(17)	3.973 (11)				

K(4) neighbor	Distance (Å)	K(5) neighbor	Distance (Å)	K(6) neighbor	Distance (Å)
O(17)^{vi}	2.770 (10)	O(7)	2.880 (12)	O(15)^{vi}	2.876 (14)
O(17)^{vii}	2.770 (10)	O(10)^{xi}	3.039 (13)	O(15)^{xiv}	2.876 (14)
O(5)	2.994 (13)	O(17)^{ix}	3.079 (11)	K(3)	2.91 (2)
O(1)^{x}	3.265 (8)	O(17)	3.079 (11)	K(2)^{xiii}	2.94 (2)
O(1)^{ix}	3.265 (8)	O(8)^{xiii}	3.092 (9)	K(1)^{xiv}	3.486 (8)
O(10)	3.36 (2)	O(8)^{i}	3.092 (9)	K(1)^{vi}	3.486 (8)
O(11)^{x}	3.362 (10)	O(13)	3.40 (2)	O(10)^{xiii}	3.57 (2)
O(11)^{ix}	3.362 (10)	O(16)^{xix}	3.449 (9)	O(9)^{xii}	3.583 (14)
O(8)^{ix}	3.841 (9)	O(16)^{xv}	3.449 (9)	O(9)^{v}	3.583 (14)
O(8)^{x}	3.841 (9)	K(4)^{xi}	3.890 (8)	O(13)	3.59 (2)
K(5)^{vi}	3.890 (8)	Next neighbor		Next neighbor	
		O(4)^{ix}	3.998 (11)	O(6)	3.895 (14)
		O(4)	3.998 (11)	O(6)^{ix}	3.895 (14)

Symmetry codes: (i) $x-\frac{1}{2}, y, -z+\frac{3}{2}$; (ii) $x, y, -z$; (iii) $-x+\frac{1}{2}, y-\frac{1}{2}, -z+\frac{3}{2}$; (iv) $x+\frac{1}{2}, y, z+\frac{1}{2}$; (v) $-x+1, y-\frac{1}{2}, z$; (vi) $x+\frac{1}{2}, y, z-\frac{1}{2}$; (vii) $x+\frac{1}{2}, y, -z+\frac{1}{2}$; (viii) $-x+\frac{3}{2}, y+\frac{1}{2}, -z+\frac{1}{2}$; (ix) $x, y, -z+1$; (x) $x, y, z-1$; (xi) $x-\frac{1}{2}, y, z+1$; (xii) $-x+1, y-\frac{1}{2}, -z+1$; (xiii) $x-\frac{1}{2}, y, z-\frac{1}{2}$; (xiv) $x+\frac{1}{2}, y, -z+\frac{3}{2}$; (xv) $-x+1, y+\frac{1}{2}, -z+1$; (xvi) $-x+1, y+\frac{1}{2}, z-1$.

and K(3)] be equal, and that combined, the four sites supplied two potassium ions per formula unit.

Owing to their strong correlation, thermal parameters and occupancies were refined in alternating cycles, with thermal parameters being refined in the final cycle. All correlation elements between thermal parameters were less than 0.5 in this final cycle. Because the electron density at the second residual peak was rather low, no atomic species was placed there. However, it is possible that this site, located at (0.6025, 0.8422, 0.4413) and which we now label Q, may serve as another interstitial position for potassium. On the other hand, without further experimentation, the possibility that water is incorporated at this, or even the K(6), site cannot be entirely ruled out.

3. Discussion of structure

3.1. Silica–neodymia framework

The structure of β-$K_3NdSi_6O_{15}$ is shown in Fig. 1. The SiO_4 tetrahedra on which the structure is based have rather typical geometries. The average $Si-O_{br}$ bond length is 1.633 (13) Å and the average $Si-O_t$ is 1.575 (9) Å. Both values lie within the range normally observed in phyllosilicates (Liebau, 1985). All terminating O atoms in β-$K_3NdSi_6O_{15}$ form bonds to a Nd atom, in addition to the one bond they form to a Si atom; the shorter $Si-O_t$ bonds, relative to the $Si-O_{br}$ bonds, reflect the stronger bonding between Si and O than between Nd and O. The fact that none of the $Si-O_t$ bond lengths are particularly large is strongly indicative of the absence of protons in the structure, which might replace some of the potassium. Such protons would be expected to reside close to terminating O atoms to form long $Si-OH_t$ bonds, as found in $K_3NdSi_3O_8(OH)_2$, for example [Hale (*sic*) *et al.*, 1993]. The average O—O separations and the average O—Si—O bond angles are also rather typical: 2.64 (4) Å and 109 (4)°, respectively. Similarly, the Nd—O distances in the NdO_6 octahedron are quite typical, ranging from 2.354 (8) to 2.400 (9) Å. This octahedron is rather distorted, however, as reflected by the wide variation in the O—O edge distances, ranging from as short as 3.105 (12) Å to as long as 4.168 (12) Å.

The basic structural features of β-$K_3NdSi_6O_{15}$ are quite similar to those of α-$K_3NdSi_6O_{15}\cdot 2H_2O$ (compare Fig. 1 of the present work to Figs. 2 and 3 of Part I of this series; Haile & Wuensch, 2000). Both structures are built on 'ideal' $(Si_2O_5)_\infty$ silica layers, in which each SiO_4 tetrahedron shares three of its oxygen ions with another tetrahedron and the fourth oxygen ion is unshared. These layers are highly corrugated and linked by corner-sharing neodymium octahedra to form a three-dimensional structure. The potassium ions (and water molecules in the case of α-$K_3NdSi_6O_{15}\cdot 2H_2O$) reside in the interstitial spaces between the silicate layers. The silicate sheets of β-$K_3NdSi_6O_{15}$ and α-$K_3NdSi_6O_{15}\cdot 2H_2O$ are shown (as they appear in the actual structures) in Fig. 2. In Fig. 3 idealized representations of these layers are depicted. Comparing Figs. 2(*a*) and 3(*a*), it is apparent that the tilting and rotation of tetrahedra in the real structure of β-$K_3NdSi_6O_{15}$ result in a doubling of the unit-cell dimension along [001] from what would be expected based on the idealized depiction. Stated alternatively, there is a pseudotranslational element of $\frac{1}{2}\mathbf{c}$ in the real structure that appears as a (true) translational element in the idealized representation. Such pseudosymmetry is not present in the layer of α-$K_3NdSi_6O_{15}\cdot 2H_2O$.

As demonstrated elsewhere, both types of silicate sheets depicted in Fig. 3 can be generated from

(i) the condensation of wollastonite-like chains, each with a triple tetrahedron repeat unit, to form xonotlite-like double chains, and

(ii) the subsequent condensation of the double chains to form layers (Haile & Wuensch, 1997).

The choice of coordinate systems (selected so that $b > a > c$, as is customary for orthorhombic systems) renders the wollas-

tonite-like chains parallel to [001] in both structures and the Si_2O_5 layers parallel to (100) in β-$K_3NdSi_6O_{15}$ and to (010) in α-$K_3NdSi_6O_{15}\cdot 2H_2O$. Both types of layers contain four-, six- and eight-membered rings. Furthermore, in both, these rings are arranged so as to form alternating rows of (6–4–6–4) rings and (8–8–8–8) rings that extend along [001], parallel to the wollastonite-like chains. The corrugation in the $(Si_2O_5)_\infty$ sheets creates hills and valleys that also extend along this direction. The extent of the corrugation in β-$K_3NdSi_6O_{15}$ is visible in Fig. 1(*a*).

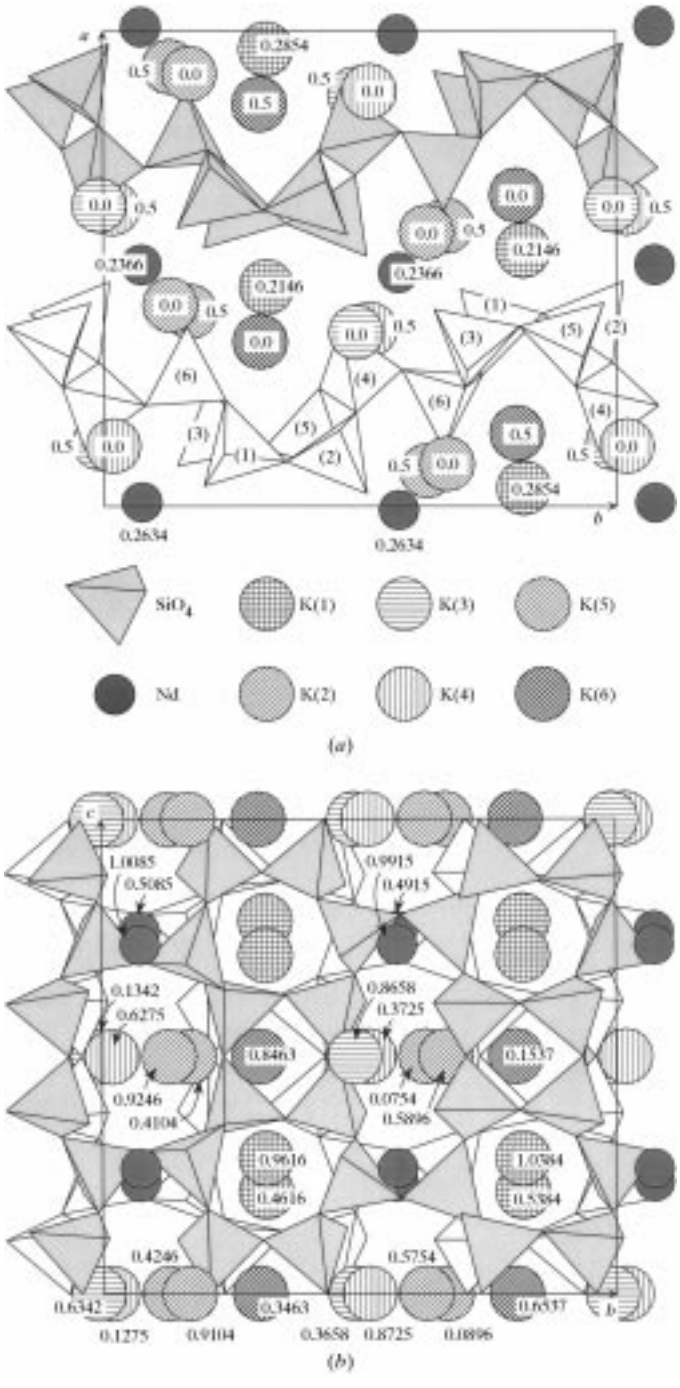

Figure 1
The structure of β-$K_3NdSi_6O_{15}$. (*a*) Unit-cell contents from $z = 0$ to $\frac{1}{2}$ are shown in projection along **c**. The remainder of the unit cell is generated by the (001) mirror plane at $z = \frac{1}{2}$. The *z*-coordinates of Nd and K atoms are as indicated. Integers in parentheses indicate the identity of the Si atom in the SiO_4 tetrahedra. (*b*) Unit-cell contents shown in projection along **a**; shading of SiO_4 tetrahedra corresponds to that in (*a*). The *y*-coordinates of Nd and K atoms are as indicated.

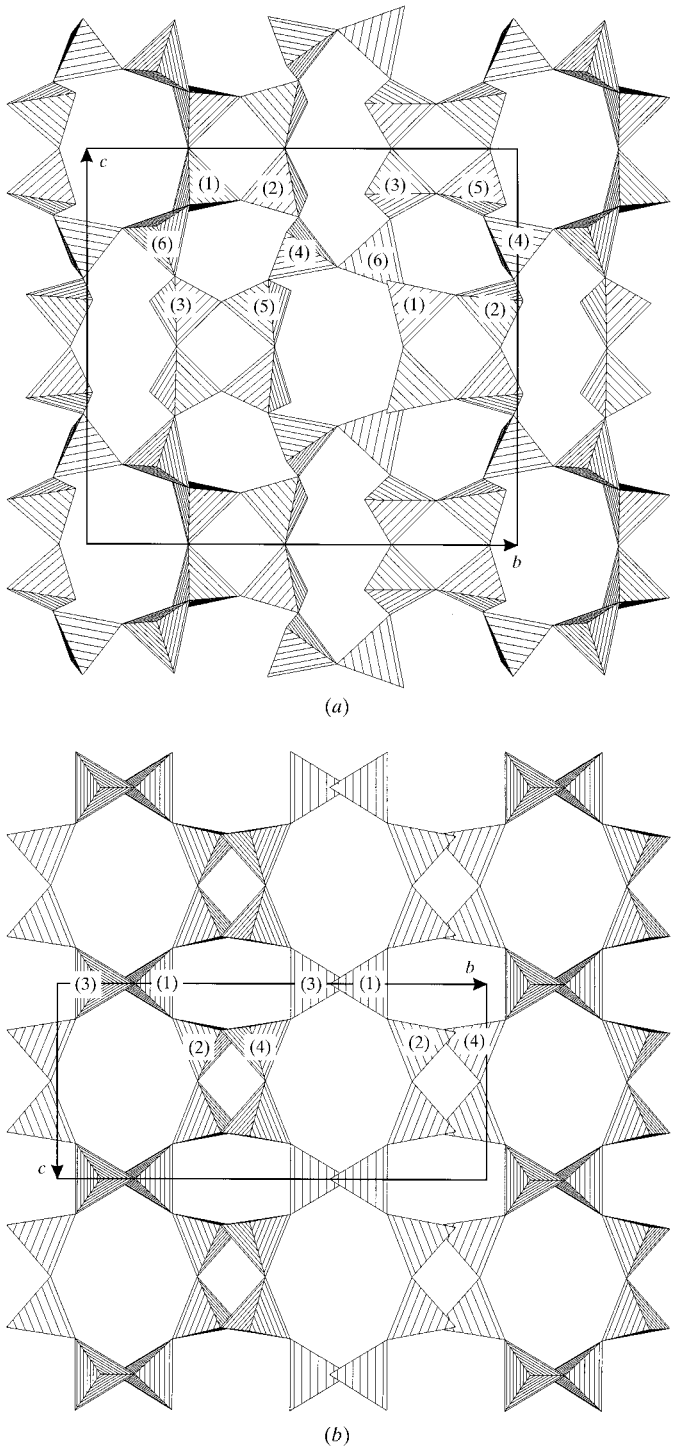

Figure 2
The $(Si_2O_5^{2-})_\infty$ layers in (*a*) β-$K_3NdSi_6O_{15}$ and (*b*) α-$K_3NdSi_6O_{15}\cdot 2H_2O$ as they appear in the actual structures. Integers in parentheses indicate the identity of the Si atom in the SiO_4 tetrahedra. A pseudotranslation operation of $0\,0\,\frac{1}{2}$ is apparent in the layer of β-$K_3NdSi_6O_{15}$.

While β-$K_3NdSi_6O_{15}$ and α-$K_3NdSi_6O_{15}\cdot 2H_2O$ share several structural features, there are significant differences between them. In addition to differences in the configuration of the wollastonite-like chains upon which they are built, the layers shown in Figs. 2 and 3 differ in the directedness of their respective SiO_4 tetrahedra, that is, whether the apical O-atom resides above the plane of the layer so as to give an 'upwards-directed' tetrahedron, or below the layer so as to give a 'downwards-directed' tetrahedron. For example, α-$K_3NdSi_6O_{15}\cdot 2H_2O$ contains some wollastonite-like chains in which all the tetrahedra are similarly directed, whereas all the chains in β-$K_3NdSi_6O_{15}$ have both upwards and downwards-directed tetrahedra.

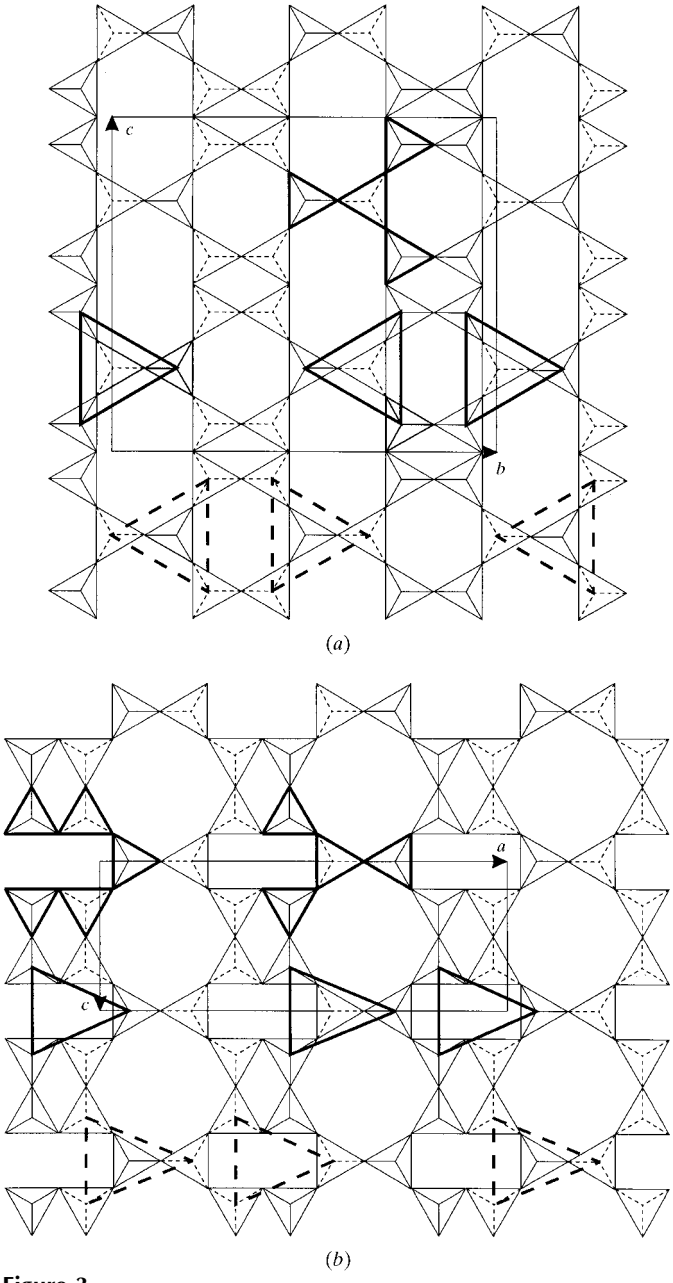

Figure 3
Idealized $(Si_2O_5^{2-})_\infty$ layers in (*a*) β-$K_3NdSi_6O_{15}$ and (*b*) α-$K_3NdSi_6O_{15}\cdot 2H_2O$. Silicate tetrahedra for which the O—O edges from bridging to terminating O atoms are drawn in solid lines have their apical O atom above the plane of the layer, whereas those for which these edges are drawn in dotted lines have their apical O atom below the plane of the layer. Several structural features are highlighted. In (*a*) an Si_4O_{13} unit is shown in the upper right-hand corner of the unit cell, three triangles that form faces of NdO_6 that lie above the layer are shown in solid lines in the lower portion of the unit cell and three triangles that form faces of NdO_6 octahedra that lie above the layer are shown in dotted lines. In (*b*) an Si_6O_{15} unit is shown in the upper left-hand portion of the figure and to its right an Si_4O_{13} unit is shown. Triangles shown in bold represent NdO_6 octahedral faces formed by these two types of silicate units to octahedra that lie above the silicate layer and those shown in dotted lines represent octahedral faces formed to NdO_6 polyhedra that lie below the layer.

The differences in tetrahedral directedness, in turn, gives rise to different types of groupings of upwards- and downwards-directed tetrahedra that are relevant to the formation of NdO_6 octahedra. In particular, β-$K_3NdSi_6O_{15}$ contains Si_4O_{13} units, an example of which is highlighted in Fig. 3(*a*), in which three outer tetrahedra are pointed in the opposite direction to that of a central tetrahedron. These Si_4O_{13} units have, as their central tetrahedron, one of the two SiO_4 groups which lie opposite one another along [010] within the six-membered rings.

In the layers of α-$K_3NdSi_6O_{15}\cdot 2H_2O$ similar Si_4O_{13} groups, as highlighted in Fig. 3(*b*), are present, however, they are formed only about the tetrahedron on the right-most side of each six-membered ring, giving rise to only half as many such groups as in β-$K_3NdSi_6O_{15}$. Moreover, a second important type of grouping, comprised of five silicate tetrahedra, is also present. This unit, highlighted in the upper left-hand corner of Fig. 3(*b*), is comprised, on its right-most side, by a tetrahedron that can also serve as the central SiO_4 group for an Si_4O_{13} unit, which is linked to two downwards-pointing ones, which in turn are each linked to an upwards-pointing SiO_4 tetrahedron.

The importance of the Si_4O_{13} and Si_5O_{16} units highlighted in Fig. 3 derive from their ability to conform to the geometry of an NdO_6 octahedron. With an appropriate degree of tilting of the three outermost tetrahedra of the unit, three terminal O atoms can be brought close enough to one another to form the face of an NdO_6 octahedron, as shown in Fig. 4. The two geometries depicted in this figure turn out to be the only ways in which NdO_6 polyhedra are linked to the silicate layers and thus can serve as a basis for understanding the three-dimensional silica–neodymia frameworks formed in these two compounds.

The locations of Nd octahedral faces within the idealized Si_2O_5 layer of β-$K_3NdSi_6O_{15}$ are shown in Fig. 3(*a*). Faces of octahedra that reside above the layer are shown as triangles with thick, solid lines and those that reside below the layer with thick, dotted lines. Each of these octahedral faces is associated with the type of Si_4O_{13} unit described earlier. Now consider the Si_2O_5 layer which resides above that depicted in Fig. 3(*a*). Although neighboring layers in the real structure of β-$K_3NdSi_6O_{15}$ are not related by simple translation along [100], they are aligned such that *n*-membered rings lie directly above one another, Fig. 1(*b*). Thus, the layers are related by pseudotranslation along [100], which for the idealized layers is equivalent to an actual translation operation. The layer placed directly above that in Fig. 3(*a*) will, consequently, have triangular NdO_6 faces on its lower side that are aligned (ignoring a

small offset along [010]) so as to cap the Nd atoms in the first layer. That is, the triangular faces drawn with dotted lines will be positioned just above those drawn with solid lines. Furthermore, the triangular faces in the original and upper silicate layers will be rotated by 180° from one another, providing the octahedral coordination observed about the single crystallographic Nd site in β-$K_3NdSi_6O_{15}$.

In the silica layers of α-$K_3NdSi_6O_{15}\cdot 2H_2O$ both Si_4O_{13} and Si_5O_{16} groups are present. The Nd octahedral faces presented by these groups are shown in Fig. 3(*b*), and again, those above the layer are drawn with thick, solid lines, and those below with thick, dotted lines. Consider, again, the layer which could be placed above that depicted in Fig. 3(*b*). If this layer were related by translation, or even pseudotranslation, to the original layer, it is apparent that any six-cornered polyhedron formed about Nd would be trigonal prismatic rather than octahedral, an unfavorable situation. Consequently, neighboring layers in α-$K_3NdSi_6O_{15}\cdot 2H_2O$ are not related by simple translation, but rather by translation and a twofold rotation operation about [001]. In this manner, neighboring layers present Nd polyhedral faces which are rotated by 180° from one another and octahedral coordination about Nd is obtained. The alignment of neighboring layers further results in Nd(1) octahedra which are capped on both sides by triangular faces formed by Si_4O_{13} groups and Nd(2) octahedra which are capped (again, on both sides) by triangular faces formed by Si_5O_{16} units. These Nd(1) and Nd(2) octahedra are arranged in an alternating manner along [100], as is evident in Fig. 3(*b*) and also along [010], the direction perpendicular to the layers.

In both structures accommodation of the geometry of NdO_6 octahedra, as shown in Fig. 4, leads to the severe corrugation of the $(Si_2O_5^{2-})_\infty$ sheets evident, for example, in Fig. 1(*a*). Taken alone the octahedra are arranged in a simple cubic array with a lattice constant of ~ 7.5 Å. The corrugation then

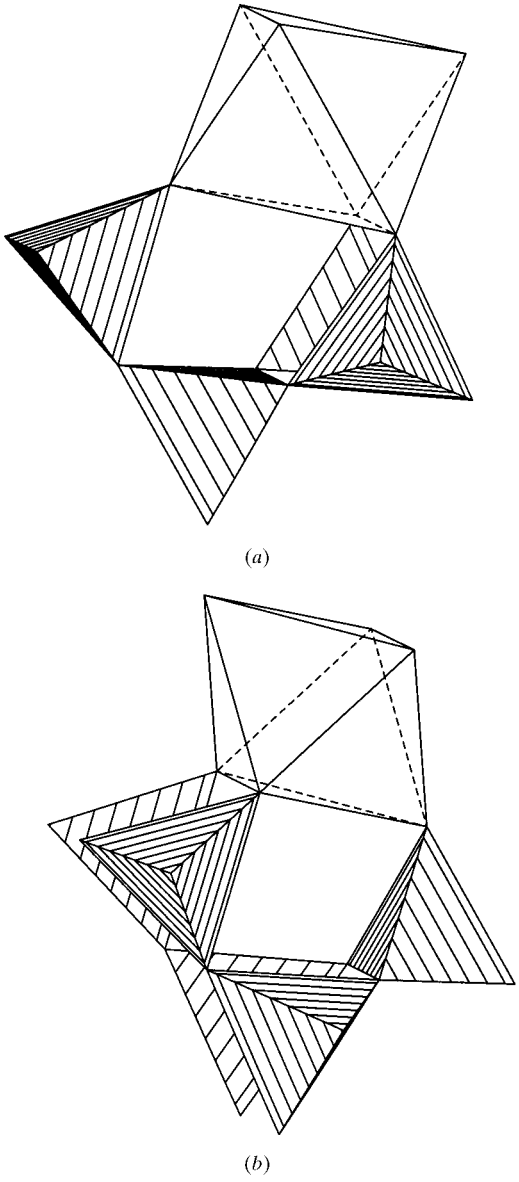

Figure 4
Local connectivity of NdO_6 polyhedra to $(Si_2O_5^{2-})_\infty$ layers. (*a*) Connectivity between an Si_4O_{13} unit and an NdO_6 octahedron, as found for all Nd atoms in β-$K_3NdSi_6O_{15}$ and for the Nd(1) atoms of α-$K_3NdSi_6O_{15}\cdot 2H_2O$. (*b*) Connectivity between an Si_5O_{16} unit and an NdO_6 octahedron, as found for the Nd(2) atoms of α-$K_3NdSi_6O_{15}\cdot 2H_2O$.

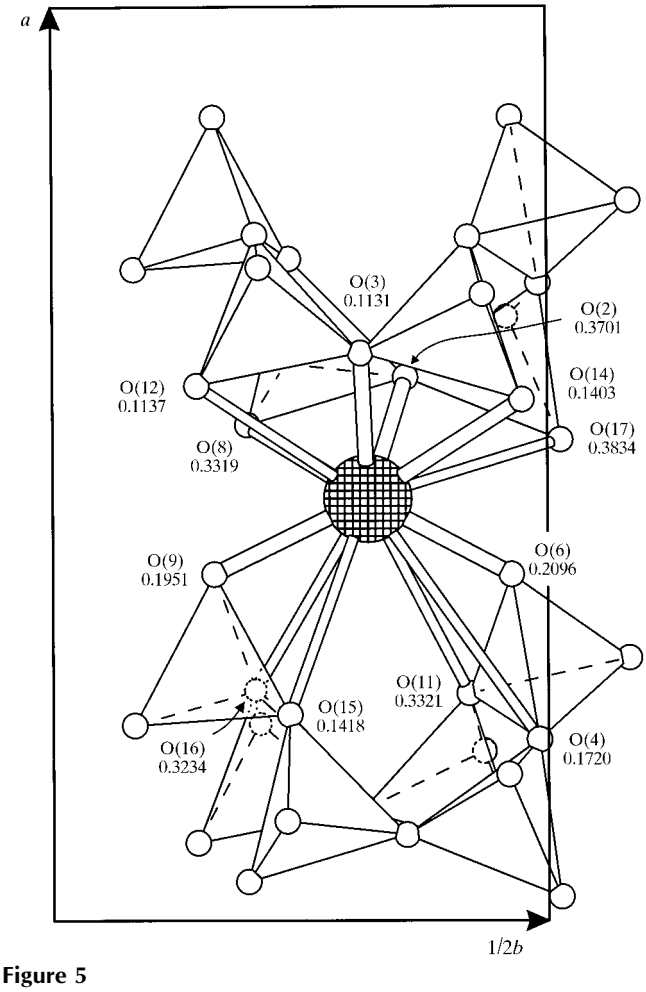

Figure 5
Projection of the structure of β-$K_3NdSi_6O_{15}$ along *c* from $z = 0$ to $\frac{1}{2}$, showing the coordination geometry about K(1) at $z = 0.2146$. The *z*-coordinate of the nearest neighbors of oxygen are indicated.

not only accommodates the local bonding geometry of the Nd octahedra, but also places the silicate layers in register with their simple cubic array. The degree of corrugation can be roughly defined as $\Delta d/d_{\rm ideal}$, where $d_{\rm actual}$ is the unit-cell dimension perpendicular to the hills and valleys created by the corrugation, $d_{\rm ideal}$ is the unit-cell dimension of the ideally flat layer and Δd is the difference between $d_{\rm actual}$ and $d_{\rm ideal}$. Assuming ideal SiO_4 tetrahedra, in which the O—O edge distance is 2.64 Å and Si—O distance is 1.62 Å, the ideal b lattice parameter of β-$K_3NdSi_6O_{15}$ is 18.29 Å. Given the actual lattice constant of 15.518 Å, the degree of corrugation is 0.152. In α-$K_3NdSi_6O_{15}\cdot 2H_2O$ the ideal a lattice parameter is 19.71 Å, corresponding to a degree of corrugation of 0.188. It is then apparent that the layers in α-$K_3NdSi_6O_{15}\cdot 2H_2O$ are more corrugated than those in β-$K_3NdSi_6O_{15}$. This result correlates with the larger volume per formula unit in α-$K_3NdSi_6O_{15}\cdot 2H_2O$ than in β-$K_3NdSi_6O_{15}$ and also with the larger repeat distance perpendicular to silicate layers in α-$K_3NdSi_6O_{15}\cdot 2H_2O$ than in β-$K_3NdSi_6O_{15}$, *i.e.* $b(\alpha$-$K_3NdSi_6O_{15}\cdot 2H_2O)$ = 15.0043 (2) Å compared with $a(\beta$-$K_3NdSi_6O_{15})$ = 14.370 (2) Å.

3.2. Interstitial species

In the structures of both β-$K_3NdSi_6O_{15}$ and α-$K_3NdSi_6O_{15}\cdot 2H_2O$ the corrugation of the $(Si_2O_5^{2-})_\infty$ sheets results in the presence of large channels in the silica–neodymia framework which extend along [001]. An additional channel is present in β-$K_3NdSi_6O_{15}$ along [100], which results from the alignment of eight-membered rings in neighboring layers. (An analogous channel is not present in α-$K_3NdSi_6O_{15}\cdot 2H_2O$ because the layers are stacked in an offset manner.)

The potassium K(1) ions of β-$K_3NdSi_6O_{15}$ reside within the large [001] channel, Fig. 1(*a*), at sites above (and below) the six-membered rings in the $(Si_2O_5^{2-})_\infty$ layers, Fig. 1(*b*). Each has 11 oxygen neighbors at distances of less than 4 Å. If one includes a rather distant O(4) at 4.695 Å, the coordination geometry about K(1) is quite regular, as can be seen in Fig. 5. It is centrally located between the two layers, with the source of its nearest neighbors equally divided between the layer above and the layer below. The K(6) ion also resides within the large [001] channel, Fig. 1(*a*), but is located above (and below) the four-membered rings, Fig. 1(*b*). Unlike K(1), it is tucked within the corrugation of one layer only, with its eight oxygen nearest neighbors deriving entirely from one layer, as is visible in Fig. 6. This figure, detailing the coordination geometry about K(6), K(2) and K(3), also reveals that these three ions form a zigzag chain that extends along [010] and conforms to the corrugation of the $(Si_2O_5^{2-})_\infty$ sheets. Much like the K(6) ion, the K(2) and K(3) ions are located in the vicinity of one or the other layer.

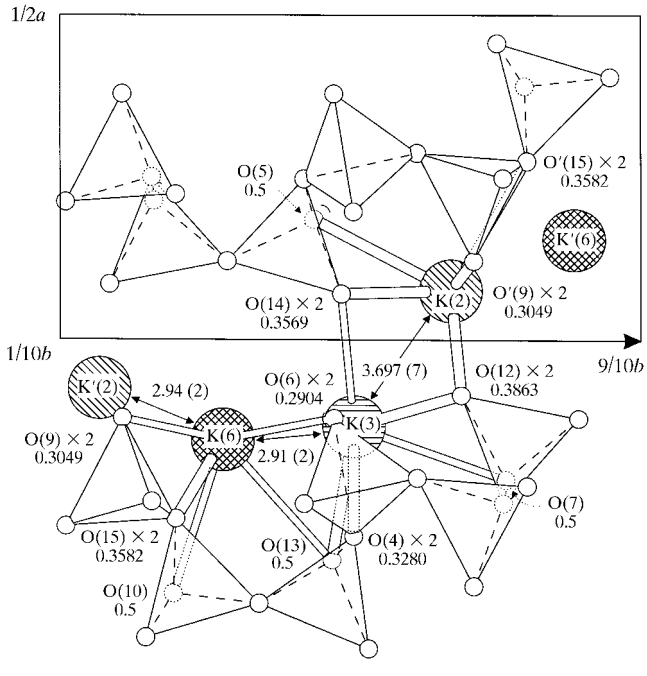

Figure 6
Projection of the structure of β-$K_3NdSi_6O_{15}$ along c from $z = \frac{1}{4}$ to $\frac{3}{4}$ showing the coordination geometry about K(2), K(3) and K(6) at $z = \frac{1}{2}$. The z-coordinate of the nearest neighbors of oxygen in the $z < \frac{1}{2}$ portion of the unit cell is indicated. Coordinates of atoms in the $z > \frac{1}{2}$ portion of the cell are given by $z' = \frac{1}{2} - z$.

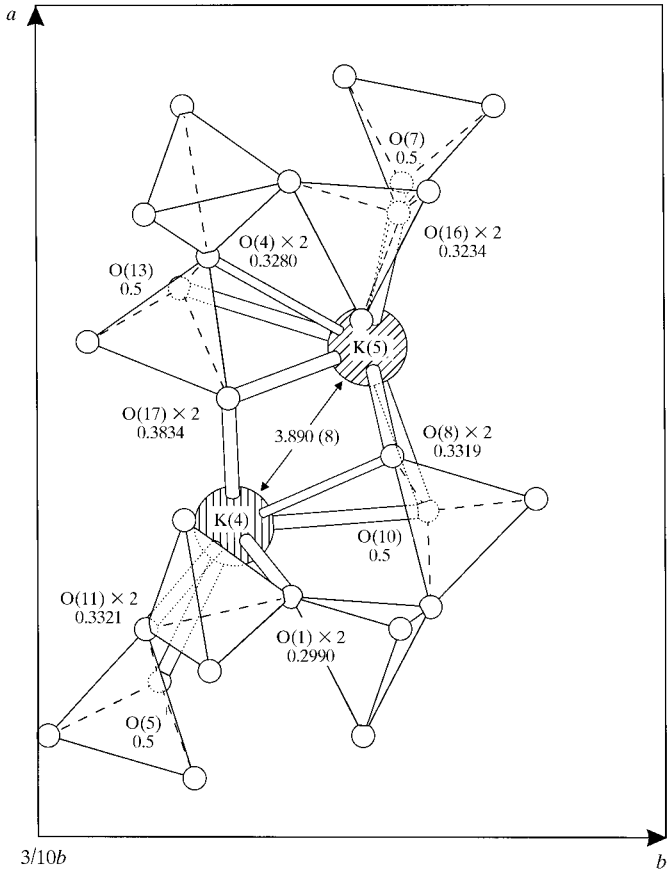

Figure 7
Projection of the structure of β-$K_3NdSi_6O_{15}$ along c from $z = \frac{1}{4}$ to $\frac{3}{4}$, showing the coordination geometry about K(4) and K(5) at $z = \frac{1}{2}$. The z-coordinate of the nearest neighbors of oxygen in the $z < \frac{1}{2}$ portion of the unit cell is indicated. Coordinates of atoms in the $z > \frac{1}{2}$ portion of the cell are given by $z' = \frac{1}{2} - z$.

The K(4) and K(5) ions reside just above (and below) the eight-membered rings, Fig. 1(*b*), in a manner that alternates with the K(2)–K(3) pair. The coordination geometry about K(4) and K(5) is shown in Fig. 7. Again, as with all but the K(1) ion, the oxygen nearest neighbors derive primarily from one layer or the other. The K(4)–K(5) ions can also be considered to form a zigzag chain that extends along [010], but in this case the distance to the next K(4) or K(5) ion (not shown in Fig. 7) is rather long, 5.464 Å. The interstitial site *Q* is located almost directly between K(4) and K(5) sites [similar to the location of K(6) relative to K(2) and K(3)]. Its distance is 2.916 Å from K(4) and 2.839 Å from K(5).

With respect to ionic conductivity, both the [001] and [100] channels present in the structure of β-$K_3NdSi_6O_{15}$ could presumably serve as pathways for ion transport. Within the large [001] channel the K(1) and K(6) sites are less than fully occupied, the distance between them is 3.486 (8) Å and no atoms in the structure directly impede a K(1) $\rightarrow$ K(6) jump. Furthermore, the U^{33} thermal vibration of K(1) is relatively large, 6.0 (2) $\times 10^{-2}$ Å^2, and, as the vector between K(1) and K(6) lies almost parallel to [0 0 1], this result suggests that the barrier to such a jump should be low.

The [100] channel contains all four remaining potassium ions, K(2)–K(5), and is shown in detail in Fig. 8. Ion transport along this pathway would involve four different types of jumps between these sites. Two of these, the K(2) $\leftrightarrow$ K(3) and K(4) $\leftrightarrow$ K(5) jumps, can be expected to be relatively easy, because each pair of sites is coordinated by face-sharing polyhedra and the sites are (pairwise) on the same side of the silicate sheets, Figs. 6 and 7. Jumps between K(2) and K(4) and between K(3) and K(5), however, may be difficult because these involve transport through the silicate layers *via* the eight-membered rings, and, not surprisingly, the jump distances are substantially longer.

The prospects for fast-ion transport along [010] are less promising than along the other two directions. Ion motion would, in this case, take place *via* the zigzag chains shown in Figs. 6 and 7. While the presence of partially occupied sites in the K(2)—K(3)—K(6) chain and a likely interstitial site, *Q*, in the K(4)—K(5) chain might lend themselves to high conductivity, the corrugation of the layers suggests that the convolution of the paths may hinder transport.

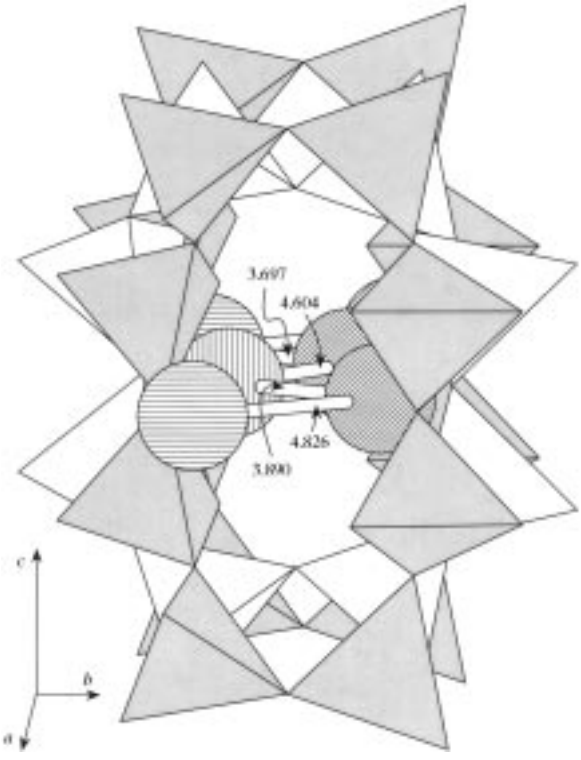

Figure 8
Location of potassium ions within a channel in the structure of β-$K_3NdSi_6O_{15}$ extending along [100] and centered at (*x*, 0.57, 0.5). The channel is formed by the alignment of eight-membered rings in $(Si_2O_5^{2-})_\infty$ layers.

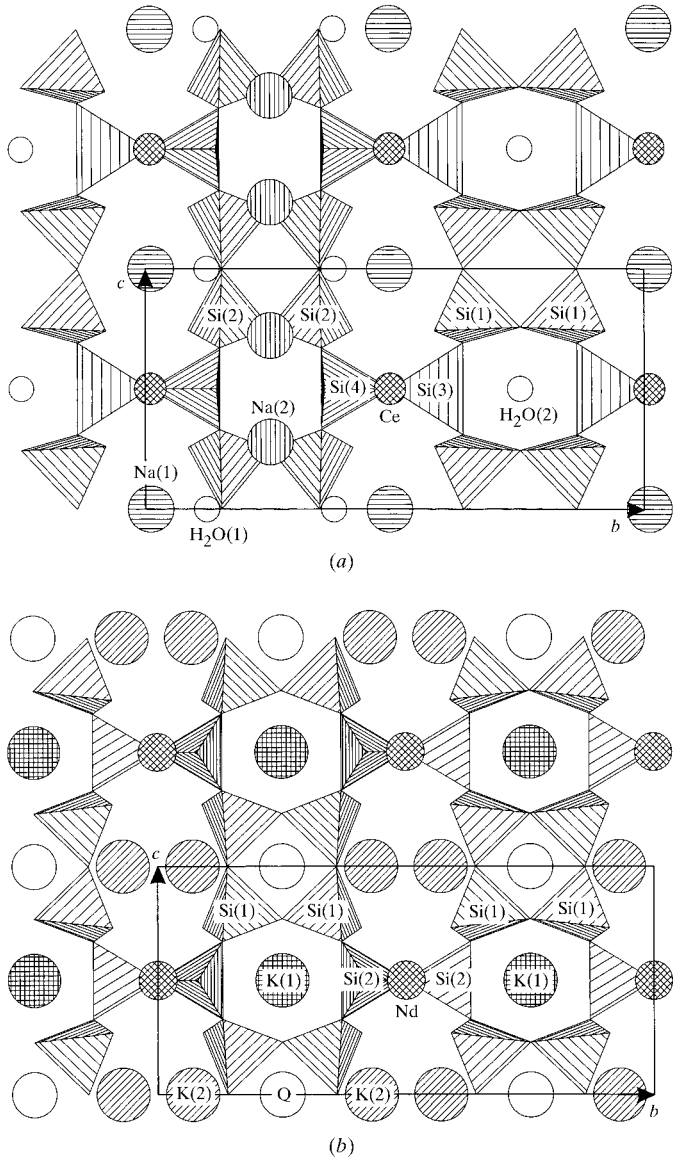

Figure 9
The structures of (*a*) sazhinite and (*b*) the proposed parent structure for both sazhinite and β-$K_3NdSi_6O_{15}$. The latter has space group *Pbmm* and assumed lattice constants of *a* = 7.20, *b* = 15.5 and *c* = 7.13 Å. (*a*) Projection along *c*; (*b*) projection along *a*.

Table 6
Coordinates of atoms in the proposed parent structure of β-$K_3NdSi_6O_{15}$ with space group *Pbmm* and unit-cell parameters $a' = \frac{1}{2}a$ and $c' = \frac{1}{2}c$ relative to the observed structure with space group $Bb2_1m$.

Atom(s)	$Bb2_1m$ position	$Z = 8$ symmetry	Atom	*Pbmm* position	$Z = 2$ symmetry	x'	y'	z'	Atom	*P2mm* position	$Z = 2$ symmetry	x	y	z
Nd	8(*b*)		Nd	2(*b*)	..2/*m*	0	1/2	1/2	Ce	2(*g*)	..*m*	0.996	0.510	1/2
Si(3), Si(5)	8(*b*)		Si(1′)	8(*l*)		0.27	0.15	0.21	Si(1)	4(*i*)		0.240	0.156	0.216
Si(1), Si(2)									Si(2)	4(*i*)		0.705	0.848	0.798
Si(4)	8(*b*)		Si(2′)	4(*j*)	..*m*	0.45	0.90	1/2	Si(4)	2(*g*)	..*m*	0.405	0.885	1/2
Si(6)									Si(3)	2(*g*)	..*m*	0.504	0.086	1/2
K(1)	8(*b*)		K(1′)	2(*f*)	2*mm*	0.92	1/4	1/2	O*w*(2)	1(*a*)	2*mm*	0.862	1/4	1/2
K(2), K(3), K(4), K(5)	4(*a*)	..*m*	K(2′)	4(*i*)	..*m*	0.20	0.57	0	O*w*(1)	2(*h*)	..*m*	0.234	0.623	0
K(6), *Q* – interstitial site	4(*a*)	..*m*	*Q*	2(*e*)	2*mm*	0.80	1/4	0						
O(1)	8(*b*)		O(1′)	2(*d*)	..2/*m*	1/2	1/2	1/2	O(8)	2(*g*)	..*m*	0.396	0.509	1/2
O(3)	8(*b*)		O(2′)	4(*k*)	.*m*.	0.2	1/4	0.23	O(1)	2(*e*)	.*m*.	0.177	1/4	0.243
O(2)									O(6)	2(*f*)	.*m*.	0.768	3/4	0.754
O(6)	8(*b*)		O(3′)	4(*j*)	..*m*	0.75	0.08	1/2	O(7)	2(*g*)	..*m*	0.724	0.061	1/2
O(9)									O(9)	2(*g*)	..*m*	0.211	0.858	1/2
O(5), O(7)	4(*a*)	..*m*	O(4′)	4(*i*)	..*m*	0.73	0.64	0	O(11)	2(*h*)	..*m*	0.623	0.652	0
O(10), O(13)									O(10)	2(*h*)	..*m*	0.312	0.363	0
O(11), O(16)	8(*b*)		O(5′)	8(*l*)		0.46	0.37	0.33	O(4)	4(*i*)		0.435	0.364	0.308
O(4), O(15)									O(5)	4(*i*)		0.513	0.648	0.671
O(8), O(12)	8(*b*)		O(6′)	8(*l*)		0.89	0.59	0.73	O(2)	4(*i*)		0.861	0.585	0.745
O(14), O(17)									O(3)	4(*i*)		0.084	0.364	0.692
									Na(1)	2(*h*)	..*m*	0.995	0.511	0
									Na(2)	2(*f*)	.*m*.	0.125	3/4	0.278

Unfortunately, none of the few crystals of β-$K_3NdSi_6O_{15}$ obtained were large enough for conductivity measurements. However, experience with related potassium neodymium silicates indicates that, while such compounds can provide useful insight into the relationship between crystal structure and ionic conductivity, they do not typically exhibit high conductivities (Haile *et al.*, 1992) in comparison to sodium-containing silicates such as Nasicon (Goodenough *et al.*, 1976) and $Na_5YSi_4O_{12}$ (Shannon *et al.*, 1978). The conductivity of α-$K_3NdSi_6O_{15}\cdot 2H_2O$, for example, is of the order $10^{-4}\ \Omega^{-1}\ cm^{-1}$ at 873 K, and, given the very close structural relationship between α-$K_3NdSi_6O_{15}\cdot 2H_2O$ and β-$K_3NdSi_6O_{15}$, it is unlikely that the conductivity of the latter should be much higher.

3.3. Pseudosymmetry and comparison with sazhinite

The structure of β-$K_3NdSi_6O_{15}$ is rather closely related to that of the mineral sazhinite (Shumyatskaya *et al.*, 1980) with approximate composition $Na_2CeSi_6O_{14}OH\cdot nH_2O$ ($n \geq 1.5$). The structure of the latter has been reported in space group *Pmm*2 and has a unit-cell volume, defined by lattice constants a = 7.50 (3), b = 15.62 (6) and c = 7.35 (3) Å, which is one quarter that of the present compound. The pseudosymmetry readily apparent in the structure of β-$K_3NdSi_6O_{15}$ (see Figs. 1 and 2*a*, for example) suggests that the phase results from a slight distortion of a structure with higher symmetry and one that, in fact, is comparable in volume to sazhinite. This higher-symmetry structure can be deduced if translation in the [100] direction is imposed on neighboring silicate layers in the $Bb2_1m$ structure or, equivalently, if a (001) mirror plane is imposed at $z = \frac{1}{4}$ (Fig. 2*a*). These symmetry operations require, for example, that Si(1) and Si(3) be crystallographically equivalent, and similarly, Si(2) and Si(5). The unit cell associated with the resulting structure is given by $a' = \frac{1}{2}a$, $b' = b$ and $c' = \frac{1}{2}c$, and its space group is $Pb2_1m$. To permit direct comparison with sazhinite, we transform the unit cell and coordinates of the sodium compound according to $a' = -c$, $b' = -a$ and $c' = b$, so as to place the silicate sheets parallel to (100) and the wollastonite-like chains parallel to [001].

The space group for sazhinite in the transformed setting is *P2mm*. Since a subgroup–supergroup relationship does not exist between $Pb2_1m$ and *P2mm*, there is not a one-to-one correlation between the atoms in the asymmetric units of β-$K_3NdSi_6O_{15}$ and of sazhinite. However, both $Pb2_1m$ and *P2mm* are subgroups of space group *Pbmm*, and the structures can easily be compared within the framework of an even higher-symmetry parent structure. In the case of β-$K_3NdSi_6O_{15}$, the parent structure can be generated by further imposing a (010) mirror plane along the interface where xonotlite-like chains meet, requiring now that Si(4) be crystallographically equivalent to Si(6), *etc*. In Fig. 9 the structures of sazhinite and the proposed parent compound, the latter generated assuming lattice constants of a = 7.20, b = 15.5 and c = 7.13 Å, are compared. These figures, projections of the respective structures along a, can, in turn, be compared to Figs. 1(*b*) and 2(*a*). The relationships between atom sites in β-$K_3NdSi_6O_{15}$, the proposed parent structure, and sazhinite are illustrated in Table 6. The origin of the parent structure is taken to coincide with the position of the Nd atom in β-$K_3NdSi_6O_{15}$ and is shifted relative to that of the $Bb2_1m$ structure by 0.075 along [010]. Accordingly, the atom coordinates in the parent phase are given by $x' = 2x$, $y' = y - 0.075$, $z' = 2z$ (where x, y and z are the coordinates in the $Bb2_1m$ structure). It is noteworthy that the partially occupied site,

K(6), and the proposed interstitial site, *Q*, become crystallographically equivalent in the *Pbmm* phase. In both Table 6 and Fig. 9(*b*), the origin of the structure of sazhinite is shifted by $(0,\frac{1}{4},0)$ from the conventional location at 2*mm* (Hahn, 1995) so as to coincide with the origin of β-$K_3NdSi_6O_{15}$ in the proposed parent phase. Relative to the coordinates given by Shumyatskaya *et al.* (1980), a total translational operation of $(0,\frac{1}{4},\frac{1}{2})$ has been applied.

From Fig. 9 and Table 6 it is apparent that while the silicate sheets in β-$K_3NdSi_6O_{15}$ and sazhinite, and even the rare-earth-silicate frameworks, are topologically identical, the structural models differ in the placement of interstitial atoms. In particular, the reported structure of sazhinite contains two alkali atoms and one proton per formula unit to balance the charge of the ceria–silica framework, whereas β-$K_3NdSi_6O_{15}$ contains three alkali atoms. Moreover, only half of the sites filled by potassium ions in the neodymium silicate are occupied in the cerium silicate and they are, in fact, reported to be filled by water molecules rather than alkali atoms. The differences between the structural models likely results from the poor quality of the data collected from sazhinite, rather than a true difference in the stoichiometries. The intensity data for sazhinite were collected photographically and the authors reported the crystal quality to be rather poor (Shumyatskaya *et al.*, 1980). While the microprobe measurements of β-$K_3NdSi_6O_{15}$ in the present work suggested a slight deficiency in potassium relative to the ideal composition, it is implausible (again, given the absence of any unusually long $Si-O_t$ bond distances) that an actual deficiency of 1 atom per formula unit exists. Moreover, the composition of sazhinite has also been reported elsewhere as $Na_3CeSi_6O_{15}\cdot nH_2O$ (Es' Kova *et al.*, 1974) and more generally as $Na_{3-x}H_xCeSi_6O_{15}\cdot nH_2O$, indicating that the uncertainty in the Na content of sazhinite is rather high. Nevertheless, the relationship between the two structures suggests that at higher temperatures their rare-earth silicate frameworks may, in fact, become isostructural, taking on the crystallographic arrangement of the proposed parent phase.

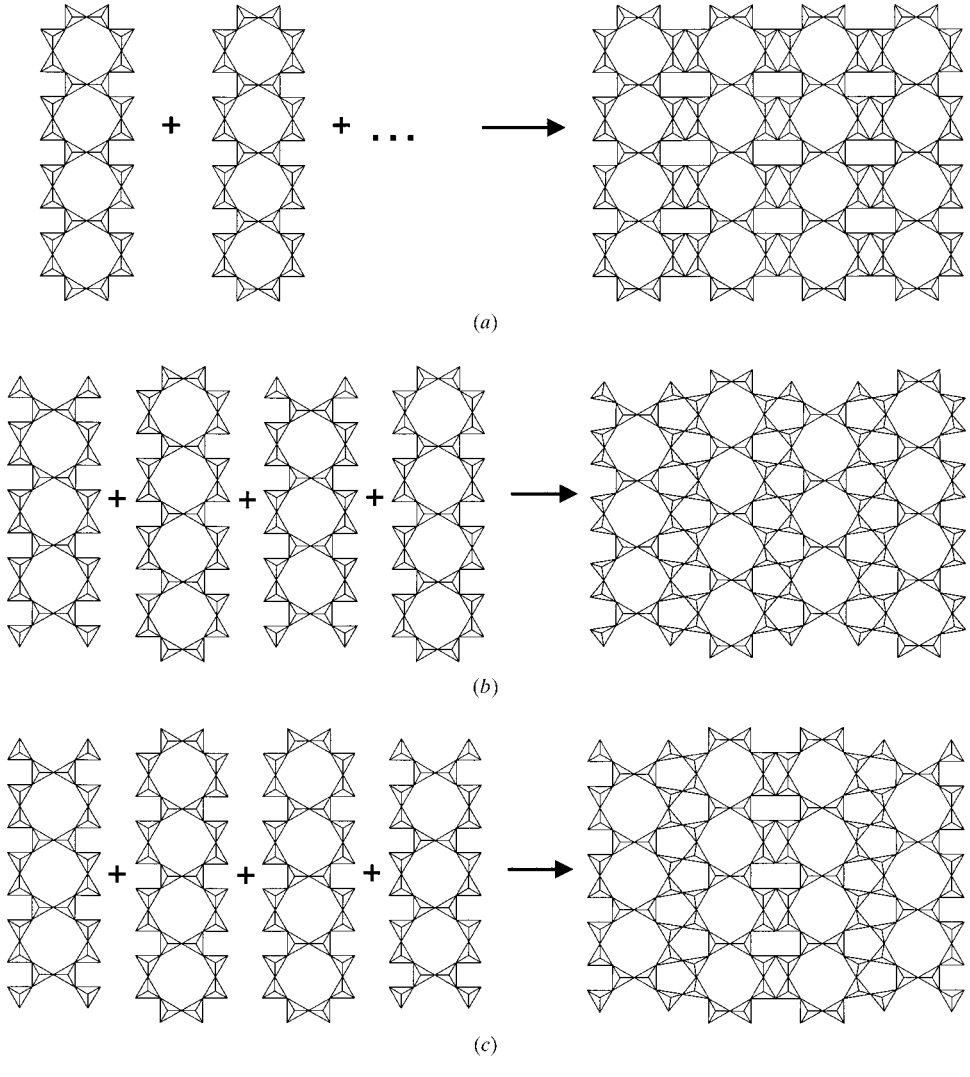

Figure 10
Linkages between xonotlite-like chains in Si_6O_{15} layers. (*a*) Condensation of chains related to one another by translation in a direction perpendicular to the chain direction; (*b*) condensation of chains after an additional translation (or shear) in a direction parallel to the chain by an amount equal to half the periodicity of the chain; (*c*) condensation of chains in an alternating manner between the direction linkages in (*a*) and the sheared linkages in (*b*).

4. On the structures of $A_nMSi_6O_{15}$ silicates

In a recent report the authors compared the structural features of $A_nMSi_6O_{15}$ silicates, where A = alkali metal or alkaline earth metal, M = Y, Ti, Zr or rare-earth metal and n = 1, 2 or 3 (Haile & Wuensch, 1997). These silicates differ from micas in that the Si_2O_5 anion does not form a flat layer. Indeed, three-dimensional framework structures, corrugated layer structures, double chain structures and structures based on isolated Si_6O_{15} units have all been observed. It is instructive to examine the structure of β-$K_3NdSi_6O_{15}$ within the context of other corrugated layer structures and also the structure of $Cs_2ZrSi_6O_{15}$ (Jolicart *et al.*, 1996), a compound which has come to the attention of the authors since the time of the publication of the original overview.

All the corrugated layer structures in the $A_nMSi_6O_{15}$ family are based on xonotlite-like double chains, as is the case for β-$K_3NdSi_6O_{15}$, although in compounds such as $K_2ZrSi_6O_{15}$ (Fleet, 1965) they may be so distorted so as to be barely recognizable. The xonotlite-like double chains may be linked together in one of three ways so as to generate the $(Si_2O_5)_\infty$ layer, Fig. 10: the chains may be linked after simple translation in a direction perpendicular to the chain extension, Fig. 10(*a*); the chains may be linked after translation in a direction perpendicular to the chain extension *and* translation in a direction parallel to the chain extension by an amount equal to half the periodicity of the chain, Fig. 10(*b*); or the chains may be linked in an alternating manner between the first two types of linkages, Fig. 10(*c*). One can imagine many more types of sheet configurations based on alternations between the 'direct' linkage illustrated in Fig. 10(*a*) and the 'sheared' linkage illustrated in Fig. 10(*b*). To date, however, only the three described here have been observed. Moreover, silicate sheets in which the xonotlite-like chains are all directly linked, as in Fig. 10(*a*), are the more common, having been reported for β-$K_3NdSi_6O_{15}$ (present work), α-$K_3NdSi_6O_{15}\cdot 2H_2O$ (Haile & Wuensch, 2000), sazhinite (Shumyatskaya *et al.*, 1980), $K_2TiSi_6O_{15}$ (Gerbert *et al.*, 1983), $K_2ZrSi_6O_{15}$ (Fleet, 1965) and $CaZrSi_6O_{15}$ (Kashaev & Sapozhnikov, 1978). The compound $Na_3NdSi_6O_{15}\cdot 2H_2O$ (Haile *et al.*, 1997) is the only known silicate to crystallize with a layer having alternating direct and sheared linkages (Fig. 10*c*), and $Cs_2ZrSi_6O_{15}$ (Jolicart *et al.*, 1996) is the only known silicate to crystallize with a layer in which there are only sheared linkages (Fig. 10*b*).

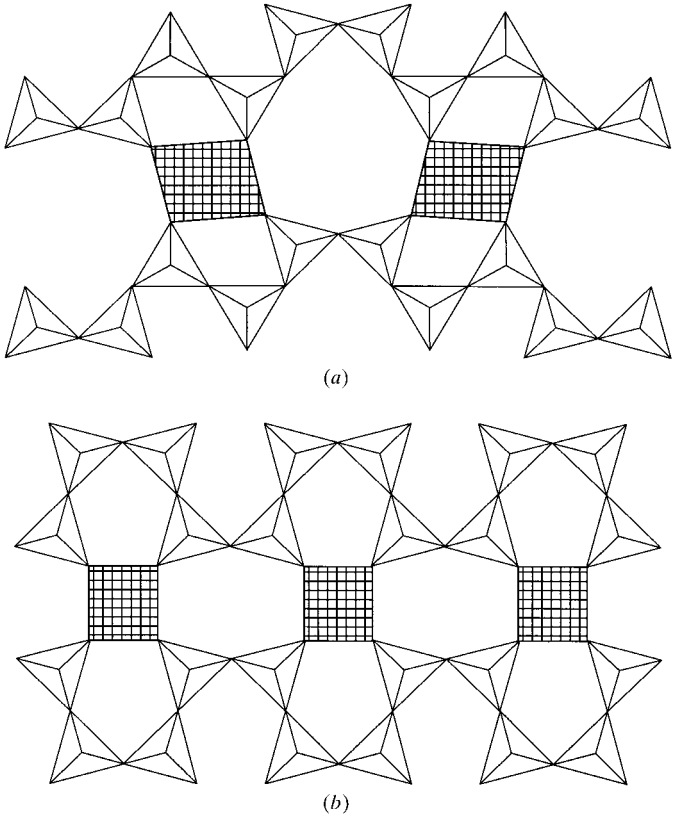

Figure 11
Schematic of the two general types of MSi_6O_{15} frameworks formed in $A_nMSi_6O_{15}$ compounds with corrugated layers. (*a*) The open frameworks encountered with large *M* cations (Nd, Ce) and (*b*) the compact frameworks encountered with small *M* cations (Zr, Ti).

It was noted in our earlier comparison of $A_nMSi_6O_{15}$ compounds (Haile & Wuensch, 1997) that the type and extent of corrugation in the layered silicates was very much dictated by the nature of the *M* cation. The large cations such as Nd^{3+} and Ce^{3+} force a corrugation that is compatible with the linkages shown in Fig. 4. Entirely different linkages are formed between ZrO_6 or TiO_6 octahedra and the Si_6O_{15} layer. Specifically, the octahedral faces of the ZrO_6/TiO_6 groups span four silicate tetrahedra as opposed to the three which the NdO_6/CeO_6 groups span, Fig. 4. This somewhat counter-intuitive feature results from the fact that accommodation of ZrO_6/TiO_6 octahedra in the manner shown in Fig. 4 would require unacceptably large strains of the Si—O—Si angles. The two general types of MSi_6O_{15} frameworks which result from the two general types of linkages with MO_6 octahedra are shown in Fig. 11. The larger *M* cations necessarily generate a framework (Fig. 11*a*) which is more open than that generated by the smaller cations (Fig. 11*b*) and that this is true regardless of the specific details of the topology of the Si_6O_{15} layer and of the nature of the *A* cation. Indeed, the compound $Cs_2ZrSi_6O_{15}$, which has a unique Si_6O_{15} layer (Jolicart *et al.*, 1996), and of which the authors had not been aware at the time these two types of frameworks were recognized, behaves in a manner that is entirely consistent with the structural picture developed. That is, the ZrO_6 octahedra in $Cs_2Zr_6O_{15}$, with an average Zr—O distance of 2.09 Å, each span four silicate tetrahedra, and the compound has an MSi_6O_{15} framework of the more compact type.

5. Concluding remarks

The new compound β-$K_3NdSi_6O_{15}$ is based on a rare-earth silicate framework which is topologically identical to that in the mineral sazhinite (Shumyatskaya *et al.*, 1980). The corrugated silicate layers that form the basis of this framework are rather similar to those of α-$K_3NdSi_6O_{15}\cdot 2H_2O$, however, differences in the directness of the tetrahedra within the layers give rise to differences in the manner in which the layers are linked to NdO_6 octahedra. In particular, the Si_2O_5 layers in β-$K_3NdSi_6O_{15}$ are linked to neodymium octahedra solely *via* Si_4O_{13} groups, whereas those in α-$K_3NdSi_6O_{15}\cdot 2H_2O$ are linked to the rare-earth octahedra *via* both Si_4O_{13} and Si_5O_{16} groups. The similarity of the hydrothermal conditions under which the two compounds were obtained suggests that the energetic differences between these types of linkages are exceedingly small. The corrugation of the silicate layers gives rise to channels within both structures. In β-$K_3NdSi_6O_{15}$ there is an additional channel that extends in the direction perpendicular to the layers because of the alignment of neighboring silicate sheets. The presence of these possible pathways for ion transport, as well as the relatively large thermal parameters of the potassium ions in β-$K_3NdSi_6O_{15}$, suggests the material might exhibit high ionic conductivity.

The authors are grateful to Karl Peters of the Max Planck Institut für Festkörperforschung for collecting single-crystal intensity data. Steve Recca of the Massachusetts Institute of Technology kindly carried out microprobe analyses. SMH thanks Joachim Maier for hosting her visit at MPI, where some portions of this research were carried out. This work is dedicated to the memory of the late Robert A. Laudise, a brilliant scientist and exemplary human being who provided invaluable guidance in the method of hydrothermal synthesis. His friendship and inspiration are greatly missed by those who were fortunate to know him.

References

Bernardinelli, G. & Flack, H. D. (1985). *Acta Cryst.* A**41**, 500–511.
Cromer, D. T. & Waber, J. T. (1974). *International Tables for Crystallography*, Vol. 4, Table 2.2A, pp. 128–134. Birmingham: Kynoch Press. (Present distributor Kluwer Academic Publishers, Dordrecht).
Es' Kova, E. M., Semenov, E. I., Khomyakov, A. P., Kazakova, M. E. & Shumyatskaya, N. G. (1974). *Zap. Vseross. Mineral. Ova*, **103**, 338–341.
Fleet, S. G. (1965). *Z. Kristallogr.* **121**, 349–368.
Gerbert, W., Medenbach, O. & Flörke, O. W. (1983). *Tschermaks Mineral. Petrogr. Mitt.* **31**, 69–79.
Goodenough, J. B., Hong, H. Y. P. & Kafalas, J. A. (1976). *Mater. Res. Bull.* **11**, 203–220.
Hahn, T. (1995). *International Tables for Crystallography*, Vol. A, pp. 208–209. Dordrecht: Kluwer Academic Publishers.
Haile, S. M. & Wuensch, B. J. (1997). *Am. Mineral.* **82**, 1141–1149.
Haile, S. M. & Wuensch, B. J. (2000). *Acta Cryst.* B**56**, 335–348.
Haile, S. M., Wuensch, B. J., Laudise, R. A. & Maier, J. (1997). *Acta Cryst.* B**53**, 7–17.
Haile, S. M., Wuensch, B. J., Siegrist, T. & Laudise, R. A. (1992). *Solid State Ion.* **53–56**, 1292–1301.
Haile, S. M., Wuensch, B. J., Siegrist, T. & Laudise, R. A. (1993). *J. Cryst. Growth*, **131**, 352–372.
Hale (*sic*), S. M., Maier, J., Wuensch, B. J. & Laudise, R. A. (1993). *Fast Ion Transport in Solids*, Proceedings of the NATO Advanced Research Workshop, pp. 315–326. Dordrecht: Kluwer Academic Publishers.
Jolicart, G., Leblanc, M., Morel, B., Dehaudt, Ph. & Dubois, S. (1996). *Eur. J. Solid State Chem.* **33**, 647–657.
Kashaev, A. A. & Sapozhnikov, A. N. (1978). *Sov. Phys. Dokl.* **23**, 539–542 (in English).
Liebau, F. (1985). *Structural Chemistry of Silicates: Structure, Bonding, and Classification*, pp. 14–16. Berlin: Springer-Verlag.
Pushcharovskii, D. Yu., Dago, A. M., Pobedimskaya, E. A. & Belov, N. V. (1981). *Sov. Phys. Dokl.* **26**, 552–554 (in English).
Schamber, F., Wodke, N. & McCarthy, J. (1981). *ZAF Matrix Correction Procedure for Bulk Samples: Operation and Program Description*, 31 pp. Tracor Northern Publications, TN-2120, Middleton, Wisconsin, USA.
Shannon, R. D., Taylor, B. E., Gier, T. E., Chen, H.-Y. & Berzins, T. (1978). *Inorg. Chem.* **17**, 958–964.
Sheldrick, G. M. (1985). *Crystallographic Computing 3*, edited by G. M. Sheldrick, C. Kruger and R. Goddard, pp. 175–198. New York: Oxford University Press.
Sheldrick, G. M. (1993). *Crystallographic Computing 6*, edited by H. D. Flack, L. Parkanyi and K. Simon, pp. 100–110. New York: Oxford University Press.
Shumyatskaya, N. G., Voronkov, A. A. & Pyatenki, Ya. A. (1980). *Sov. Phys. Crystallogr.* **25**, 419–432 (in English).